Journal of Materials Science and Engineering A 2 (11) (2012) 693-711

Corrosion Resistance of Steel/Zinc with Silicate Nanoparticles/Polyurethane Paint Systems in NaCl Solution

Célia Regina Tomachuk[1], Cecilia Inés Elsner[2] and Alejandro Ramón Di Sarli[3]

1. Energy and Nuclear Research Institute, IPEN/CNEN-SP, CCTM, 2242, CEP 05508-000, Cidade Universitária, São Paulo, SP, Brazil

2. CIDEPINT: Research and Development Center in Paint Technology (CICPBA-CONICET), Av. 52 s/n entre 121 y 122. CP. B1900AYB, La Plata-Argentina

3. Engineering School, National University of La Plata, Av. 1 Esq. 47. CP. B1900TAG, La Plata-Argentina

Received: September 28, 2012 / Accepted: October 16, 2012 / Published: November 10, 2012.

Abstract: Surface characteristics and corrosion behaviour of bare electrogalvanized steel coated with polymer/nano-silicate particles added to the electrogalvanizing bath were studied by scanning electron microscopy (SEM), energy dispersive spectrometer (EDXS) and electrochemical impedance spectroscopy (EIS). After applying a barrier polyurethane paint, the paint hardness, porosity, flexibility, colour, gloss, blistering and rusting degrees, and anticorrosive protective properties in 0.05 mol·L^{-1} NaCl solution were also evaluated. The results correlated well and, being demonstrative of the very slow deterioration rate of the immersed coated electrogalvanized steel, they enabled to assume that if a chemically analogous but thicker coating system was applied; it could be an acceptable alternative in real service conditions.

Key words: Electrogalvanized steel, conversion treatment, EIS, corrosion, nano-scale filler, polyurethane paint.

1. Introduction

Electroplated zinc coatings are utilized as active galvanic protection for steel. In order to this protection is effective longer, it should be taking into account that factors such as temperature, pH, current density and zinc ions concentration of the galvanizing bath, and the physicochemical characteristics of the substrate surface influence the mechanism of zinc electrodeposition. As well, the addition of organic and/or inorganic additives to the electrolytic baths is very important because they may be active not only on the coatings growth and structure but also making them smooth and shiny. Accordingly, the added organic particles and/or oxides such as silica can be adsorbed on the cathodic surface changing the activation energy and charge transfer rate of the electrochemical reactions controlling the electrocrystallization mechanism

Zinc coatings are electrochemically very reactive and, consequently, high corrosion rates are found in internal as well as external atmospheres [1]. This reason makes necessary applying a post-treatment to increase their useful life. In current industrial practice, this treatment consists of the plated zinc immersion in a chemical bath for depositing a conversion layer. This last is a dielectric passive layer with high corrosion resistance and also provides a better surface for paint adherence. The main problem of traditionally used post-treatments is the presence of Cr^{6+} salts, considered toxic and carcinogenic substances whose usage is forbidden by European regulations [2].

Corresponding author: Alejandro Ramón Di Sarli, doctor in engineering, research fields: corrosion, protection by organic and/or inorganic coatings, new materials. E-mail: ardisarli@gmail.com.

Chemicals based on trivalent chromium [3-5], molybdates [6, 7], tungstates [8], permanganates, vanadates, zirconium salts [9-11], cobalt salts [12], organic polymers [13, 14], rare earth salts doped with silane [15-19] and carboxylates [20] are some alternatives being tested for the Cr^{+6}-based anticorrosive layers replacement.

Many recent studies have been focused on improving the corrosion resistance of non-toxic Cr^{+3}-based conversion layers either applying sealing treatments and/or adding different additives to the bath [4]. However, trivalent chromium compounds such as Cr_2O_3 and $Cr(OH)_3$ could oxidize to hexavalent chromium under certain conditions [21]. Consequently, it could be argued that the development of new conversion treatments should derive towards chromium-free and ecologically acceptable products. Nevertheless, the formulation, fabrication technology and corrosion behaviour of these coatings are still not clear and their practical effectiveness are doubtful.

In this context, inert fillers have been developed to improve desirable properties of protective coatings such as adhesion and anticorrosive protection. As well, it is important to remark that inorganic fillers, as for example the silicate materials, present some advantages: (1) large surface area and adsorption capacity; (2) the chance of controlling adsorption properties; (3) channels and cavities in the range of many molecules; and (4) molecule identification by the unique pore structures. Taking into account these characteristics and that the zinc polymer coatings offer greater anticorrosive protection than the electrogalvanized layer acting alone, those found an interesting field of application in the automotive industry. Such an enhancement was attributed to the synergy between the zinc galvanic protection and the polymer presence. Besides, the surface quality (controlled texture, uniformity) of products coated with a zinc polymer layer not only make them particularly useful to fabricate main body visible pieces that have to satisfy severe aesthetic requirements after painted but also it strengthens the paint adherence.

In line with the purpose of improving the zinc corrosion resistance, it should be noted that when this metal is protected by a painting system, its dissolution rate is related to the transport of corrosion inducing species (oxygen, ions) through the paint layer, the charge transfer and/or delamination processes at the metal/coating interface as well as to the composition-structural changes of the paint layer [22]. Moreover, the coated metal performance depends on the metal surface preparing, polymeric material, interfacial adhesion, environmental aggressiveness as well as of the coating crosslinking degree, continuity, thickness and composition [23].

The organic coatings applying on conversion layers are required for producing structures where the zinc layer long-lasting is addressed. This process implies to apply one or more coats of paint on the metallic surface, and then a drying/curing period under, preferably if possible, environmentally controlled conditions [24-29]. The production and applying processes of these polymeric materials usually causes volatile organic compounds (VOCs) emissions, which involve serious environmental and public health problems. European standards impose limits to the VOCs use and emission in industrial zones where painting cycles are working, reason by which the development of waterborne paints started to be considered [30-45]. These products basically differ from the traditional paints in that the organic solvent content is less than 10% (w/w), but they offer excellent stability, small size particles, can be pigmented using appropriated products, and are compatible with a large variety of additives and curing agents. Besides, once the paint film has cured gives very high hardness and good abrasion resistance [44]. Other remarkable characteristics are that generally provide thin thickness by coat, therefore, the film homogeneity and continuity could probably be critical parameters. Nevertheless, this kind of problem can be easily overcome by applying more coats.

In this context, modified polyurethane paints are widely used due to their good hardness combined with excellent adhesion to metallic substrates, anticorrosive properties and weather resistance [46-49]. For all these reasons, such paints have been studied by several authors, who determined variations of coatings pores resistance, coatings dielectric capacitance, polarization resistance, double layer capacitance [50-52], and also the relationship between electrolyte diffusion through the paint coat and the corrosion resistance of the underlaying metal [53, 54].

Selection of anticorrosive schemes for the protection of steel pieces creates serious problems to both the pre-treatments formulators and the painting system designers. When more details about the coating scheme itself and the substrate as well as the interactions between them are available, higher is the chance to get the best formulation for each practical situation. As a general rule, the coatings corrosion behaviour is evaluated using traditional essays such as Salt Spray Chamber [55], Kesternich [56], and/or Saturated Humidity Chamber [57], but the faster and objective information about the corrosion reactions kinetics provided by the electrochemical methods is also very important.

The present work is part of an ongoing research program performed at CIDEPINT focused to elucidate physicochemical phenomena occurring within and under paint coatings, encompassing defects in films, porous films, metal/coating adhesion, surface treatment and/or pre-treatment's, corrosion, blistered coatings and cathodic protection. A large amount of diverse data has been gathered using standardized tests as well as electrochemical techniques, and then interpreted on the basis of their correlation with a number of physicochemical processes that occur in the complex coated steel/exposure medium interface.

The surface morphology, structure and composition of electrogalvanized steel sheets containing nano-scale filler (SiO_2) in the zinc coating were characterized by SEM and EDXS. Then, their corrosion performance was evaluated in 0.05 mol·L^{-1} NaCl solution by EIS [58, 59]. Replicates of these samples were painted with an environmentally friendly barrier topcoat polyurethane paint, and both the physicochemical properties of the dry paint film and the anticorrosive performance of the whole system immersed in the same chloride containing solution for 69 days were assessed.

2. Experiments

2.1 Samples

AISI 1010 steel sheets (7.5 cm × 10 cm × 0.1 cm) industrially electrogalvanized (zinc layer 10.46 ± 0.22 μm thick) using a composite coating (ZPOL®), based on an acid Zn plating bath added with a polymer containing silicate nanoparticles (10 nm average size and specific area 600 $m^2 \cdot g^{-1}$) kindly supplied by ArcelorMittal, were used as metallic substrates. Electrodeposition was carried out galvanostatically at a cathodic current density of 2 A·dm^{-2} and a temperature of 22 ± 3 °C. Replicates of those electrogalvanized steel sheets under the same operation conditions but without addition of the composite coating were used as bare reference samples.

Prior to be painted, the electrogalvanized panels were extensively cleaned with acetone, ethanol and distilled water to remove any surface contaminant. Finally, they were coated with a barrier topcoat polyurethane-based paint pigmented with TiO_2 (rutile) and micronized silica mesh 325. The particle size distribution, from 0.1 to 10 μm, was checked according to the ASTM D 1210-(2010) standard [60]). The paint components, characteristics and application method are summarized in Table 1.

2.2 Characterizations

2.2.1 Morphological Analysis

The characterization of the pre-treated electrogalvanized steel (ZP) samples morphology was accomplished by Scanning Electron Microscopy (SEM) using a Philip model SEM 505 with ADDAII system,

while its composition was determined using Energy Dispersive X-Ray Spectroscopy (EDXS) with a Si detector and 20 keV energy.

2.2.2 Thickness Measurements

The thickness of the bare (Zn) and pre-treated (ZP) zinc layers was measured by the X-Ray fluorescence method (ASTM B568-2009 standard) using the Helmut Fischer mod. XDL-B equipment, while the corresponding to the dry paint film (ZPP samples) was measured according to the ISO 2808: 2007 standard using the Elcometer 300 coating thickness gauge. The thickness uniformity was evaluated by SEM of cross-sections after samples' cracking in liquid nitrogen.

2.2.3 Polyurethane Paint Film

After the curing process, the following tests were carried out:

Metal/paint adhesion: adhesion measurements were carried out using Tape Test based on the ASTM D 3359-09e2 standard [61].

Porosity: it was evaluated according to the ASTM D 5162-08 standard [62] by using the Elcometer 236 DC Holiday Detector; maximum applied voltage = 2,500 V.

Gloss and colour: were respectively determined according to the ASTM D 523-08 [63], and the ASTM D 2244-11 [64] standards by using the BYK Gardner Spectro-Guide Sphere Gloss with 60° of incidence angle.

Hardness: it was accomplished according to the ASTM D 3363-11 standard [65].

Flexibility: the 3.2 mm mandrel (equivalent to 28% of elongation) was chosen to perform this test according to the ASTM D 522-93a-08 standard [66]. One layer of the PU paint was applied on pre-treated steel panels and kept in laboratory atmosphere (RH 65% ± 5% and 23 ± 2 °C) for 7 days.

Blistering and rusting degrees: the size and frequency of blisters as well as the white rusting degree were evaluated according to the ASTM D-714-02/09 and ASTM D-610/08 standards, respectively [67].

2.2.4 Electrochemical Behaviour

On each coated steel sample, and separated by a distance of 1-1.5 cm, two cylindrical tubes of transparent acrylic were fixed by means of an epoxy adhesive to get good adhesion to the substrate. The EIS measurements were carried out using a conventional electrochemical cell with the three-electrodes arrangement, where the counter and reference ones were respectively a Pt-Nb mesh and a Saturated Calomel Electrode (SCE), and the working electrode was the coated steel sample, placed horizontally looking upwards at tha bottom in a flat-cell configuration. Defined area = 15.9 cm^2. All the measurements were performed at 22 ± 3 °C in open to the air 0.05 $mol \cdot L^{-1}$ NaCl solution.

Impedance spectra in the frequency range $10^{-1} < f$ (Hz) $< 10^5$ were performed, in the potentiostatic mode at the corrosion potential (E_{corr}), as a function of the exposure time in the electrolyte solution with a Solartron 1255 FRA® coupled to an Impedance Potentiostat-Galvanostat Omnimetra PG-19A® and both controlled by the ZPlot® program. The rms amplitude of the sinusoidal voltage signal applied to the system was 8 mV, and 10 points per decade were registered. The experimental spectra were fitted to model equivalent electrical circuits by using the Boukamp software [68], and the circuit components were laterly associated to the physicochemical process occurring in the system. All impedance measurements were executed with the electrochemical cell inside a Faraday cage to reduce external interferences as much as possible. The samples integrity was checked by measuring the corrosion potential after all the tests to confirm that the change from the initial value was no higher than ± 5 mV.

Besides, the water diffusion, solubility and permeability coefficients of the painting system were determined just after immersion in the 0.05 $mol \cdot L^{-1}$ NaCl solution. For this, the dielectric capacitance evolution was measured as a function of the immersion time until a constant value was attained. Such measurements were performed with the same equipment arrangement described above, in the

potentiostatic mode and at a frequency of 2×10^4 Hz. The coefficients value was estimated by using a method reported elsewhere [69].

Taking into account that the corrosion behaviour of passivated, painted and/or multi coated materials strictly depends on the production procedure, all the tests were carried out on three replicates of each sample type and the average results obtained for them are the reported in the following tables and figures.

3. Experimental Results

3.1 Characterization of Zn and ZP Samples

Information related to the coatings morphology after the coating/drying process is highly significant since the presence of flaws such as pores, cracks, and/or other coating defects could produce areas were localized corrosion of the metallic surface starts from its exposure to a given environment [70, 71].

The morphology of the pre-treated surface was observed by SEM at up to a maximum of 1,000 × (Fig. 1a) and 10,000 × (Fig. 1b). As seen in Fig. 1a, the entire surface of ZP samples exhibits small spheres shaped particles which have a strong tendency to agglomerate, while the image in Fig. 1b shows the layer homogeneity and the presence of inorganic fillers within the zinc coating.

As presented in Fig. 2, semi-quantitative elemental analysis made by SEM/EDXS on ZP samples surface

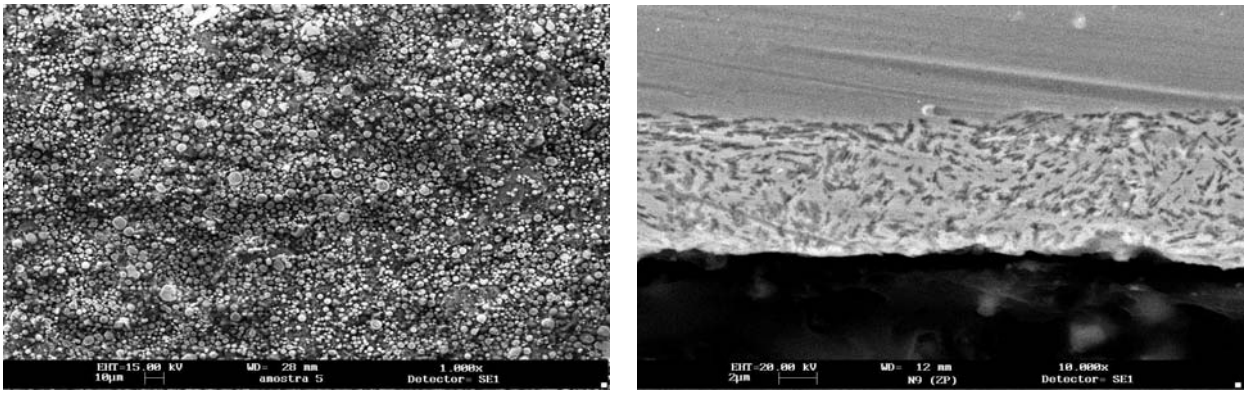

(a) surface (b) cross section

Fig. 1 The SEM micrograph of the ZP sample as-received: (a) surface and (b) fractured cross section.

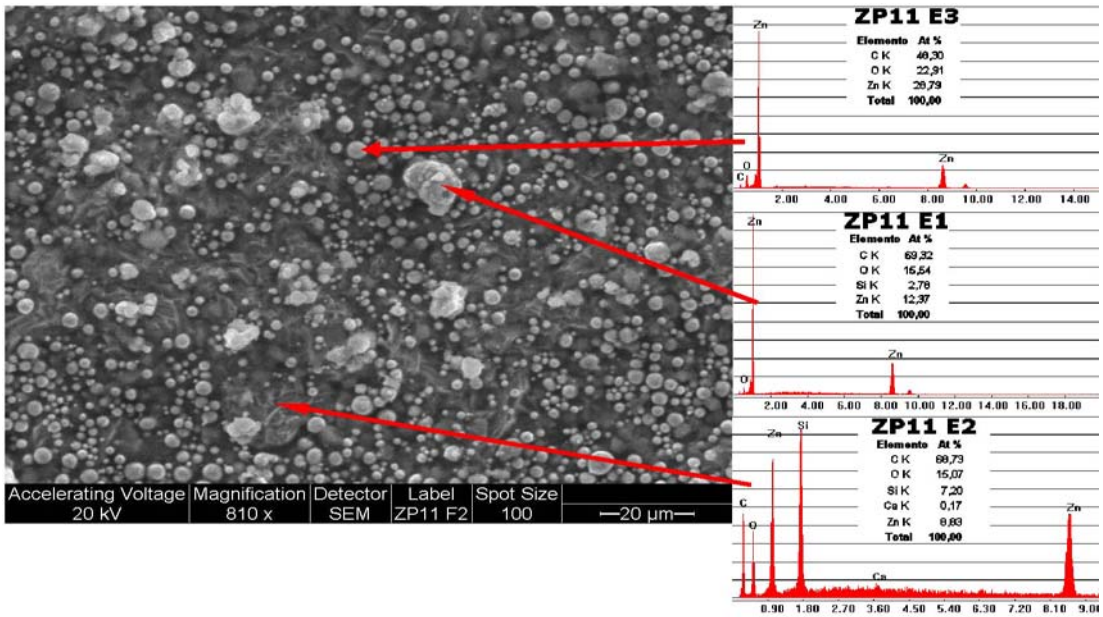

Fig. 2 EDXS profile of the ZP sample.

indicated that the coating composition was zinc, silicon particles and other elemental impurities. Besides, from both Figures can be certainly inferred that the silicon particles added to the zinc bath for improving the coating tribological behaviour were dispersed within the polymeric matrix. The ZP layer average thickness estimated from the SEM of the cross sections was found to be about 12 ± 2 μm.

3.2 Results of the Standardized Tests Carried Out on the Dry Paint Film Before and After the Exposure to the 0.05 mol.L^{-1} NaCl Solution

3.2.1 Adhesion

Different studies have shown that in many cases the loss of adhesion is coincident with the presence of water at the metal/coating interface [59, 72, 73]. In the rather qualitative tape-test the scales used by the ASTM D-3359/09 standard to classify the specimens is from 0 B to 5 B, where 0 B corresponds to a very poor (percent of area removed greater than 65%) and 5 B to a very good adhesion (percent of area removed 0%), respectively. In the present case, once concluded the curing process of the polyurethane paint film, the pre-treated and painted electrogalvanized steel sheets (ZPP samples) were subjected to immersion in 0.05 mol·L^{-1} NaCl solution for 69 days. At the end of these, the panels were re-inspected and classified.

Before the immersion, the adhesion value was 5B, and after that it was 4B (percentage of area removed < 5% inside and outside the cell). This minor adhesion loss (delamination) at the paint/zinc interface could be attributed to the break of chemical bonds between the polymer layer and the zinc surface, an effect known as "wet adhesion". Such an effect has been related to rearrangements in the membrane structure due to the pressure of the water uptake [73] as well as to the strongly dielectric character of water which acts like a plasticizer and can modify the intermolecular cohesive forces. This is an extremely important effect in anticorrosive coatings since water, oxygen and ionic permeation increases as the glass transition temperature *(Tg)* decreases.

3.2.2 Gloss and Colour

Gloss measurements at 60º angle of observation performed before and after the immersion did not show noticeable changes. The average values were, respectively, 85 and 81.2, which indicate that the paint film behaved as a gloss of perfect white diffuser. Since this property is associated to the smoothness of the paint film, the slight decreasing was probably due to small changes of the polyurethane surface texture as a consequence of the water absorbed during the immersion. As well, the polyurethane film colour did not show any change in its chromaticity values.

3.2.3 Porosity

Before and after de immersion no pore was detected at 2500 V. This means that the entire surface of the paint film exhibited a suitable continuity, which was not modified by the test conditions.

3.2.4 Hardness

The polyurethane film hardness was determined in terms of pencils leads of known hardness. Before and after the immersion test, the measurements gave values harder than 6H, which specify a paint film classified as hard, property that did not change despite the aggressive exposure conditions.

3.2.5 Flexibility

The immersion of the painted samples in 0.05 M NaCl solution for 69 days gave rise to important changes in the stiffness of paint film. Before the immersion, the polyurethane paint film behaved satisfactorily since after bending no cracking, checking or flaking was observed but, at the end of the exposure, that underwent cracking. This change in the polyurethane film performance was ascribed to the fact that, as the exposure test elapsed, the paint film drying (crosslinking) process carried on leading to an increase of the paint film stiffness, which became more brittle.

3.2.6 Blistering and Rusting Degrees

The visual inspection made on replicates of the painted electrogalvanized steel panels suggests that a highly effective corrosion inhibitive action was

developed by the barrier polyurethane paint. After 69 days exposure to aerated 0.05 M NaCl solution, the average values for blistering and rusting degrees were 10 and 10 which, according to the respective ASTM standards [67], pointed out that no one of the ZPP samples subjected to immersion evidenced any deterioration signal able to be detected by naked eye.

3.3 Electrochemical and Corrosion Behaviour

The barrier properties of painting systems are of great interest since they determine the water transport and/or dissolution and supply of pigments to the metal substrate. Water permeability and ionic diffusion as well as corrosion potential and impedance measurements provide insight related with those organic coating properties. In such sense, the heterogeneous nature of the electrical properties of polymeric films is physically represented as an also heterogeneous group of electrolitically conducting paths. Thus, in localized areas, the polymer does not behave like a dielectric but shows an electrolytic conductivity due to electrolyte dissolution within structural defects (free volume) of the polymer or as a consequence of its penetration through the film pores. In other localized regions, the coating has the properties of a relatively inert dielectric material. At the metal/organic coating interface, several complex processes of difficult interpretation may take place since after the corroding species (H_2O, O_2 and ionic species) permeation different electrochemical reactions are possible [74, 75].

When painted and pre-treated steel plates are submerged in an aqueous solution, the water absorbed by the organic coating can dissolve some pigments. It is known that a high barrier effect or a low diffusion of corrosion inhibiting species can keep or accelerate the active state even if there is a significant pigment content in the paint film. Thus, it is difficult to determine whether the metallic substrate is passivated or not, particularly in the presence of anions like Cl^-, which are capable of breaking the passivating layer [76, 77]. This can be only balanced either by increasing the minimum anticorrosive PVC required to obtain such layer [76, 78, 79] and/or the paint film barrier properties using a properly chosen painting system.

3.3.1 Water Permeability

An ideal paint film should be impervious to penetration by both water and chemicals. However, as this type of film does not exist in practice, from the paint film concerns, barrier and permeability properties are of great interest because they control the corrosive chemicals transport through it as well as the active pigments dissolution and supply to the metal substrate. Reliable data on water permeability, corrosion potential and impedance evolution of coated metals provide valuable information to select and design the most adequate protective paint system for each practical situation.

The value of water permeability coefficient was estimated from measurements of the parallel capacitance as a function of the immersion time [69] using a linear regression of the Carpenter equation [80], which defines the amount of absorbed water as follows:

$$\frac{d\varphi}{dt} = 8D\,\frac{(\varphi_\infty - \varphi_0)}{d^2}\cdot e^{(-\pi^2 D/d^2)t} \qquad (1)$$

Where, t, immersion time of the paint film (s); Φ, amount of water absorbed by the paint film at the time t, (g); Φ_∞, amount of water absorbed by the paint film at t = ∞, (g); Φ_0, amount of water absorbed by the paint film at t = 0, (g); d, paint film thickness, (cm); D, diffusion coefficient, ($cm^2 \cdot s^{-1}$).

According to Ritter, et al. [81], it may be assumed that different amounts of water, oxygen and ions can permeate the coating in the first hours of immersion in saline solution. This process is explained by considering that the relatively small water molecules can permeate the organic coating and form hydrogen bonds with other water molecules in either liquid or solid state, as well as with polar groups present in materials with which they are in contact. Hence, water absorbed in the coating can form hydrogen bonds with hydrophilic or polar groups of the polymer and

permeation is followed by the spatial movement of water from high to low pressure levels. Part of the energy necessary for this movement is supplied by the thermal motion of the polymer molecules. As different polymers also have different mobility, the water faces different degrees of resistance in permeating through them. This resistance is related to the cross-linking degree in the polymer as well as to the penetrating molecule size. In a highly cross-linked product the randomness due to the movement of chain segments and the formation of free spaces is restricted, reducing the diffusion rate and consequently the permeation of the absorbed species.

Taking these concepts into account, in permeability measurements the random values of the impedance vector after 15-20 min immersion are probably related to rearrangement in the membrane structure due to the pressure of the water uptake as well as to the strongly dielectric character of water which acts like a plasticizer and can modify the intermolecular cohesive forces [73]. This is particularly very important in anticorrosive coatings since water, oxygen and ionic permeation increases as the glass transition temperature **(**T_g**)** decreases.

In the present work, an approach to the barrier properties of the polyurethane paint film took place by estimating its water diffusion (D), solubility (S) and permeability (P) coefficients, which are associated to the mobility of the water molecules (diffusion) and the amount of water dissolved within (i.e., at the free volume) the coating (solubility). The obtained average values were: $D = 5.48 \times 10^{-10}$ $cm^2 \cdot s^{-1}$; $S = 0.036$ (Adimensional); and $P = 1.95 \times 10^{-11}$ $cm^2 \cdot s^{-1}$.

By comparing these results with those reported elsewhere [69], it may be assumed that the whole polyurethane layer was intact, continuous and highly crosslinked.

3.3.2 Time Dependence of the Corrosion Potential (E_{corr})

Fig. 3 illustrates that just after immersion in the 0.05 $mol \cdot L^{-1}$ NaCl solution, the corrosion potential (E_{corr}) of Zn samples shifted quickly towards more negative values due to the surface layer of ZnO dissolved leaving the more reactive zinc particles exposed to the electrolyte. Then, the continuous but slight changes of the E_{corr} towards more positive observed from the first day of immersion may be ascribed to a decreasing of the $[Zn^{2+}]$ in the electrolyte solution caused by the fact that the deposition rate of Zn^{2+} as oxide/hydroxides was somewhat greater than its production from the zinc dissolution reaction. In other words, such an increase started when the white corrosion products deposited on the zinc layer where dense enough as to diminish the zinc dissolution rate.

With regard to the ZP samples, Fig. 3, the initial E_{corr} value of about -1.02 V/SCE shifted to about -0.98 V/SCE after 6 hours immersion, and then moved slowly up to reaching -1.08 V/SCE. This evolution shows that at the beginning of the test, the E_{corr} of the ZP samples was about 0.040 V more negative than that of the Zn samples but, after 6 hours, the displacement of both potentials was quite similar up to the end of the respective tests, i.e., 12 and 3 days of exposure. Therefore, at first glance and based only on this result would be possible to infer that the nanosilicate particles addition to the electrogalvanizing bath did not improve the corrosion performance of the zinc layer.

The time dependence of the corrosion potential (E_{corr}) values measured for painted metals has been questioned with regard to its use as a technique for

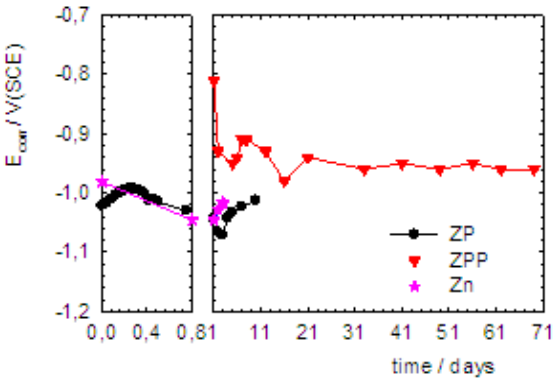

Fig. 3 Evolution of E_{corr} of Zn, ZP and ZPP samples at selected immersion times in aerated 0.05 $mol \cdot L^{-1}$ NaCl solution.

evaluating the anticorrosive resistance of organic coatings [82]. However, its changes as a function of the exposure time to aqueous media have been successfully used as a simple tool to study the corrosion protection afforded by organic coatings [83-85]. Depending upon the microstructure of the paint coating, especially its polymerization degree, a certain period elapses until electrolyte penetration channels are established through which the underlying metal comes into contact with the medium. So, it is not surprising that, when a compact structure and high crosslinking level are accompanied by an also high film thickness, a few days of testing is not enough time for the electrolyte to enter in contact with the base metal of coated specimens, form the electrochemical double layer, and enable the measurement of a corrosion potential.

Fig. 3 shows the corrosion potential (E_{corr}) values measured for the ZPP samples exposed to 0.05 mol·L^{-1} NaCl solution. As can be seen, the Ecorr value measured just after immersion was about -0.8 V/SCE, but after 1 day it shifted at about -0.92 V/SCE, a value near to the measured for the Zn and ZP samples, even though for the ZPP samples it remained almost constant during the whole test. This means that, at least from the thermodynamic point of view, the protective properties offered by the paint layer were not enough as to avoid the water diffusion until the surface of the underlaying metallic substrate.

3.3.3 Impedance Spectra

As first stage, a comparative analyses of the EIS spectra coming from the bare (Zn), pre-treated (ZP) as well as pre-treated and painted (ZPP) electrogalvanized steel samples immersed in naturally aerated 0.05 mol·L^{-1} NaCl solution was performed on the basis of complex plain (Nyquist) and Bode diagrams. Fig. 4 illustrates the EIS spectra corresponding to the three samples type exposed for 3 days, while Fig. 5 presents the Nyquist plots for the ZP and ZPP samples at longer (and selected) exposure times.

Just after the exposure, the EIS plots of the Zn samples show two time constants more or less well defined, as depicted in Fig. 4. Then, as the exposure time elapsed, they tended to overlap entirely indicating that the relaxation processes took place at the same time and, consequently, only one flattened semicircle could be observed. However, as it will be after discussed, each flattened semicircle could contain more than one time constant (τ) since they overlap when the $\tau_i/\tau_{i+1} < 5$ [86]. Besides, such semi-circle flattening also provides an indication of the surface roughness in such a way that being this perfectly smooth appears as a perfect semi-circle and the sphericity decreases with increasing roughness [87, 88]. According to this, it can be assumed that as the zinc dissolves in the test solution, the surface profile become progressively more irregular. Some authors [89-91] reported that the zinc dissolution process involves a reversible step with an intermediate Zn (I) species adsorbed on the zinc surface and its further oxidation giving soluble Zn (II) [92].

Taking into account that the maximum impedance (|Z|) values for ZP samples were less or equal than 1×10^3 Ω at the lowest frequency, an increase of its corrosion resistance would be highly desirable. With this purpose, silicate nanoparticles were added to the electrogalvanizing bath.

The result of such addition was the ZP samples, whose EIS plots are also shown in Fig. 4 for 3 days of immersion. As can be seen, from the beginning of the test at least two time constants were well defined, and the maximum impedance value at the low frequency limit of the corresponding spectra was slightly greater than that for the Zn samples.

The comparative tests for 3 days of exposure were completed by using the electrogalvanized steel/polyurethane paint system (ZPP), Fig. 4. In this case, the Nyquist diagrams showed very large slopes with an almost vertical to the horizontal axis, while the Bode diagram displayed straight lines with the slope close to 1. An impedance value greater than 1×10^8

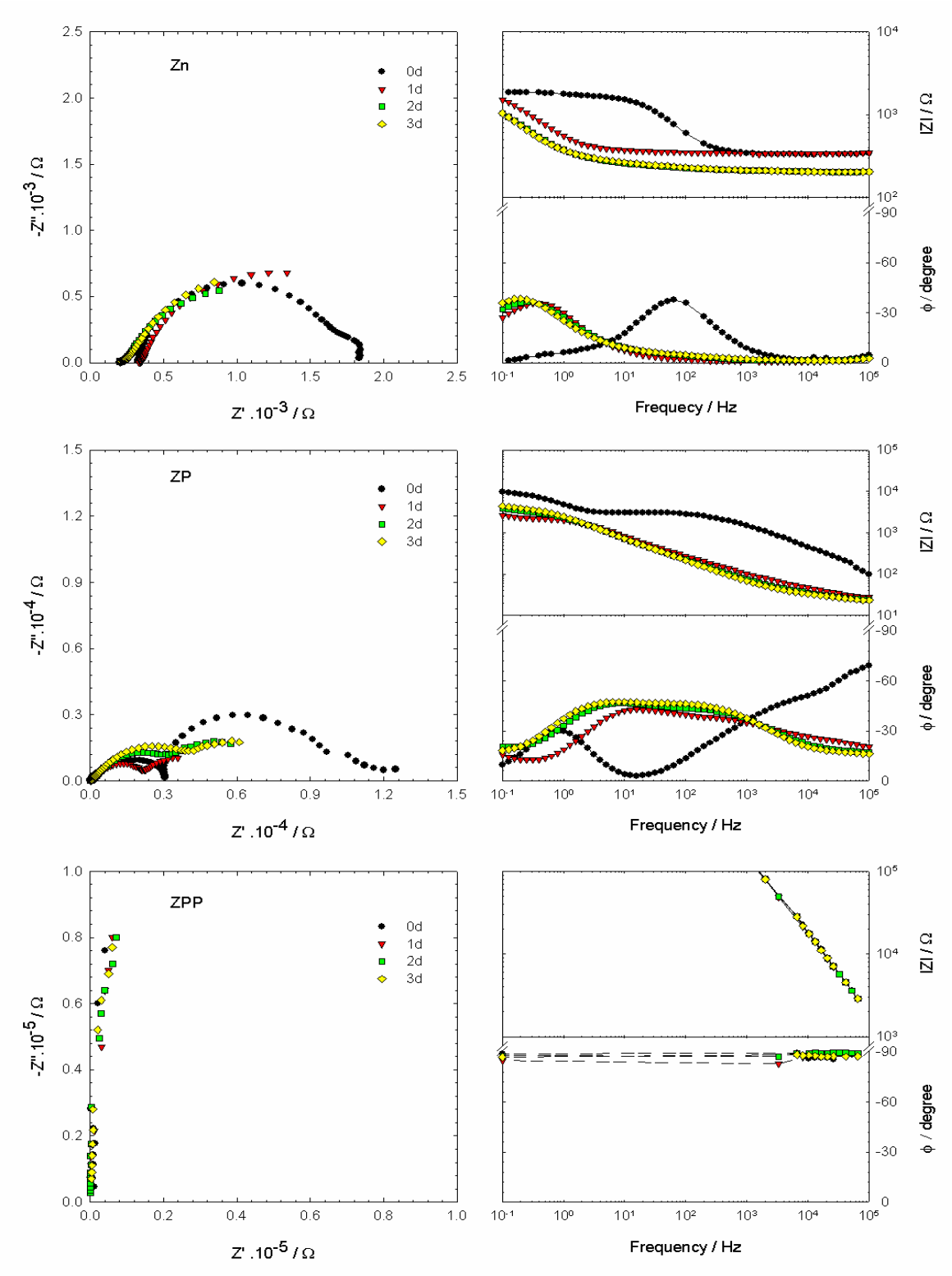

(a) (b)

Fig. 4 Representative Nyquist (a) and Bode (b) diagrams of the Zn, ZP and ZPP electrogalvanized steel samples for 3 days immersion in aerated 0.05 mol·L^{-1} NaCl solution.

$\Omega \cdot cm^2$, and a phase angle close to 90º for nearly all the frequency range covered in the measurement, shows at this time an effective insulating layer of paint and, hence, a well protected metallic substrate.

The immersion test was followed up to 12 days for the ZP samples (see inset in Fig. 5), and 69 days for ZPP samples, Fig. 5. The Nyquist diagrams corresponding to the ZP samples showed two clearly separated time constants at 5 and 12 days, but certain overlapping of them at 7 days exposure. Likewise, for the ZPP samples can be seen that the purely capacitive behaviour, characteristic of a highly effective barrier film, remained without significant changes up to 21 days of immersion, time at which a well defined capacitive loop was observed. As the time went on, the radius of the semicircle in Nyquist plots decreased. This shows that the dielectric capacitance of the paint film increased gradually due to electrolyte permeation and, as a result, the protective performance reduced.

3.3.4 Equivalent Circuit Models

The underlaying pre-treated electrogalvanized steel as well as the painting system deterioration has a complex nature, consequently, to interpret and explain in electrochemical terms the time dependence of the acquired impedance data, it has been necessary to propose the equivalent circuit models shown in Fig. 6a-c. Each equivalent circuit corresponds to the parallel and/or series connection of resistors and capacitors simulating a heterogeneous arrangement of electrolitically conducting paths. In the three equivalent circuit models required by the present study, R symbolized the electrolyte resistance between the reference and working (coated steel) electrodes, but the remaining electrical and electrochemical resistive-capacitive parameters forming part of the transfer function derived from the most probable equivalent circuit [68] used in each case were associated to different interfacial processes [28, 93-96].

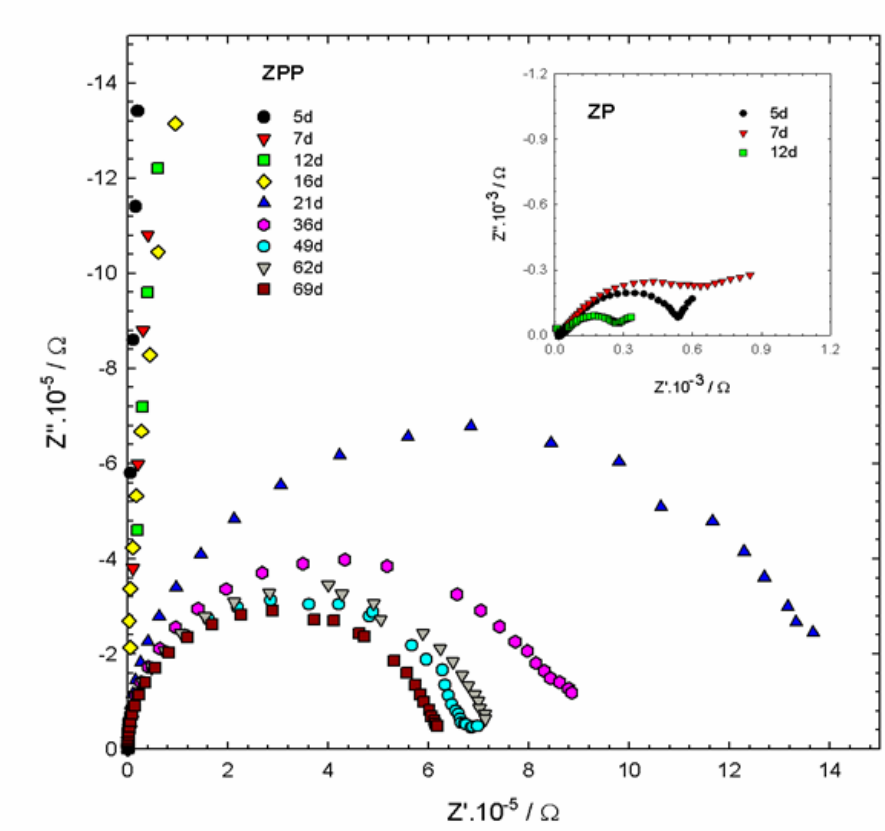

Fig. 5 Representative Nyquist diagrams of ZP and ZPP samples for selected immersion times in aerated 0.05 mol·L^{-1} NaCl solution.

Hence, for fitting the impedance spectra of Zn samples the circuit shown in Fig. 6a was used, where R_t represented the charge transfer resistance and C_{dl} the electrochemical double layer capacitance related to the faradic process, while the couple R_1C_1 was the contribution of the dissolution reaction intermediates to total impedance of the working electrode. In the case of ZP samples, Fig. 6b, R_c characterized the pre-treatment layer resistance to the electrolyte diffusion and C_c the dielectric capacitance of the intact part of the same film. Once the permeating and corrosion inducing chemicals (water, oxygen and ionic species) reach electrochemically active areas of the substrate, particularly at the bottom of the coating defects, the zinc corrosion become to be measurable so that its associated parameters, C_{dl} and R_t as well as the couple R_1C_1, associated to the contribution of the dissolution reaction intermediates to the overall impedance of the working electrode, can be estimated. Finally, in the model used for fitting the ZPP samples impedance data, Fig. 6c, R_c represented the polyurethane paint plus the polymeric coating resistance to the electrolyte diffusion and C_c the dielectric capacitance of the intact part of the same film, while the couple R_tC_{dl} were related to the underlying zinc corrosion [97, 98].

Distortions observed in these resistive-capacitive contributions indicate a deviation from the theoretical models in terms of a time constants distribution due to either lateral penetration of the electrolyte at the electrogalvanized steel/paint interface (usually started at the base of intrinsic or artificial coating defects), underlying galvanized steel surface heterogeneity (topological, chemical composition, surface energy) and/or diffusional processes that could take place along the test [74, 75]. Since all these factors make the impedance/frequency relationship to be non-linear, they are taken into consideration by replacing one or more capacitive components (C_i) of the equivalent circuit transfer function by the corresponding constant phase element Q_i (CPE), whose impedance dispersion relation is given by [28, 68]:

$$Z = (j\omega)^{-n}/Y_0, \text{ and } n = \text{CPE power} = \alpha/(\pi/2) \quad (2)$$

Difficulties in providing an accurate physical description of the occurred processes are sometimes found. In such cases, a standard deviation value ($\chi^2 < 5 \times 10^{-4}$) between experimental and fitted impedance data may be used as final criterion to define the most probable circuit.

According to the impedance spectra dispersion, the fitting process was performed using either the dielectric capacitance C_i or the phase constant element Q_i, however, the C_i parameter was used in the following plots to facilitate the results visualization and interpretation.

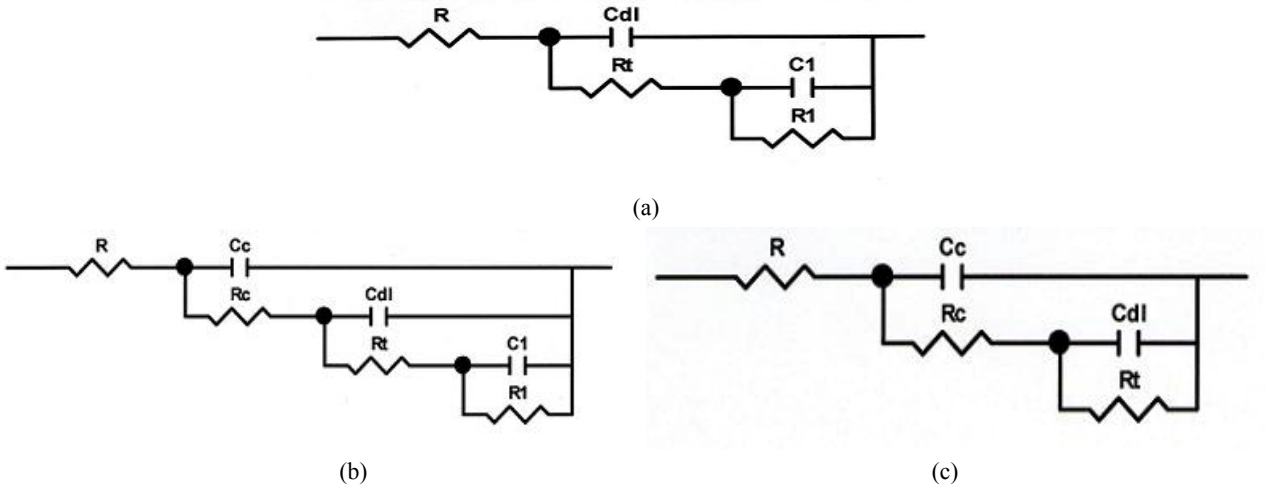

Fig. 6 Equivalent circuits for the fitting of, (a) ZP and (b) ZPP samples during their immersion in aerated 0.05 mol·L^{-1} NaCl solution.

3.3.5 Time Dependence of the Impedance Resistive-Capacitive Components

According to the bibliography [99, 100], the interpretation of the impedance spectra shown in Fig. 4 for the Zn samples support the existence of an anodic dissolution mechanism in two stages involving the presence of at least one reaction intermediate. From the proposed equivalent circuit, the samples' performance can be evaluated in terms of R_t values, which are inversely proportional to the corrosion rate. In addition, taking into account the transfer function derived from the equivalent circuit model, the magnitude of the total resistance corresponding to the impedance value extrapolated to frequencies tending to 0 of the zinc dissolution reaction occurring in two stages is given by $R_t + R_1$, i.e., the resistance R_p measured with DC technique [101].

Fig. 7a presents the time dependence of R_t values for Zn samples. As can be seen for the first day of immersion, such values were stable and not too low (≅ 1.10^4 Ω·cm^2), possibly due to the presence of a ZnO layer, and this evolution was in agreement with the slight variation of the E_{corr}. As the time elapsed, it increased to about 6×10^4 Ω·cm^2 but at the third day decreased to about 1×10^3 Ω·cm^2; in both cases the E_{corr} shifted towards more positive and close to the initial values, between -1.04 and ≈ -1.00 V/SCE. Therefore, the initial tendency suggests that neither the corrosion rate nor the electrochemically active area of the zinc layer changed significantly during the first day of immersion probably due to the presence of a ZnO layer covering the zinc particles. After 1 day of immersion, R_t started a slow increase mainly because: a) the active surface became totally covered by precipitated corrosion products (zinc oxides and hydroxides) with lower electrical conductivity than that of the electrolyte, and/or b) the adsorption of these products in detriment of the dissolution reaction intermediates, which, associated with the coverage degree of the reactive surface, influence the behaviour of both the R_t and R_1

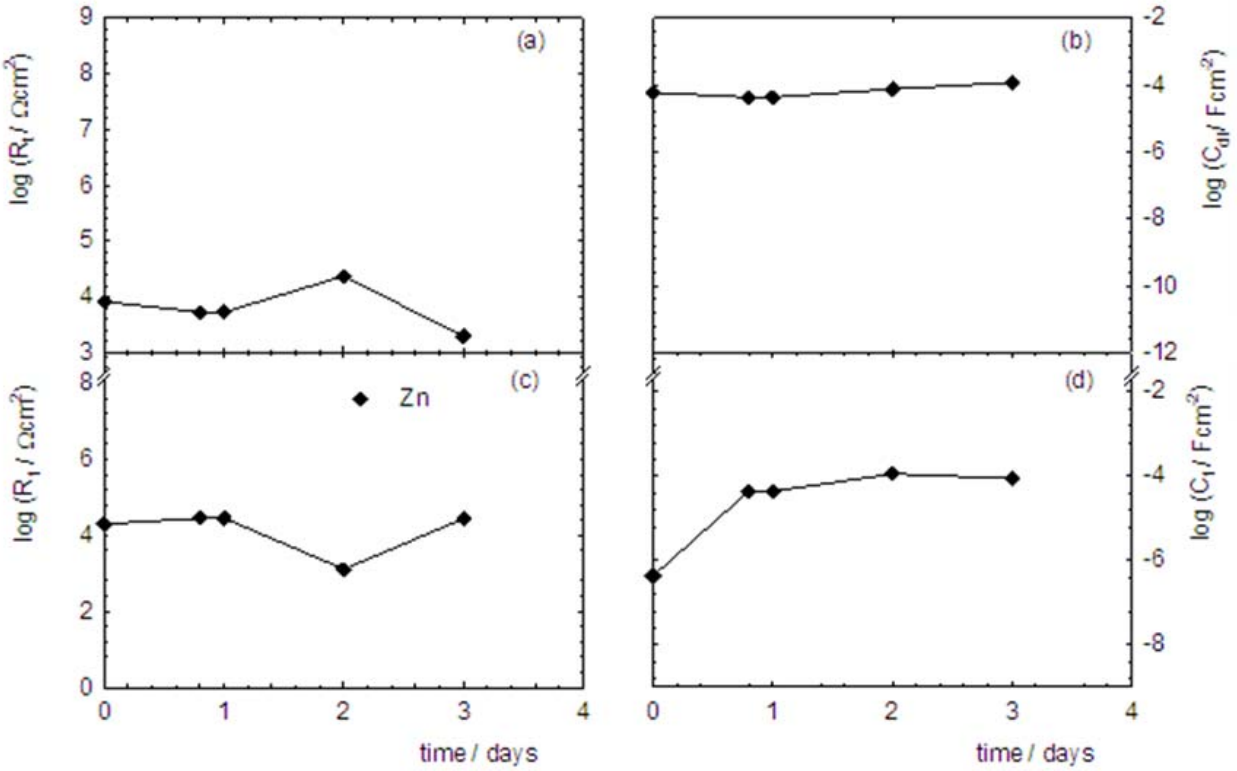

Fig. 7 Evolution of (a) logR_t, (b) logC_{dl}, (c) logR_1, (d) logC_1, impedance parameters of Zn samples at selected immersion times in aerated 0.05 mol·L^{-1} NaCl solution.

(Fig. 7c) resistances. The subsequent decreases of R_t could be explained in terms of the dissolution of new and electrochemically unstable localized surface areas, which, in turn, led to an increase of the adsorption intermediates concentration and, as a result, of R_1.

The variation of the electrochemical double layer capacitance (C_{dl}) values for 3 days of immersion is represented in Fig. 7b. During all this time this capacitance remained stable and close to 1×10^{-4} F·cm^{-2}. The fact that the values of these two parameters depend inversely (R_t) and directly (C_{dl}) on the electrochemically active area size, but their changes did not follow linearly such a dependence could be explained assuming that both parameters would be affected by slightly different areas [98] due to the zinc dissolution reaction was coupled to the absorption-desorption processes of the reaction intermediates.

On the other hand, the C_1 evolution (Fig. 7d) would be associated to a competitive effect between the fluctuation rate of the sorption area size and the thickness of the products involved in this process. According to this hypothesis, just after immersion, the adsorption area increased faster than the adsorbed layer thickness, therefore C_1 increased but then, when the layer became thicker, compact and dense making that the reaction area was limited to the size of the electrochemically active surface, both rates reached a quasi-equilibrium enabling that C_1 remained almost constant.

Fig. 8a illustrates that at the first day of exposure the resistance (R_c) of the ZP samples decreased quickly, while the coupled capacitance (C_c) increased quickly due to the electrolyte solution permeating the pores of the thin coating matrix covering the zinc layer. However, from the end of the day R_c increased while C_c increased. Then, as the immersion time went on, both parameters showed a fluctuating evolution for the 12 days of testing. Changes in R_c values could be explained in terms of blockage of the coating pores by accumulation of zinc corrosion products (R_c increases), and the periodical appearance of new conducting paths in less resistant areas of the coating (R_c decreases). On the other hand, the fluctuations observed in C_c values are related to water absorption-desorption of water in the free volume within the pre-treatment layer structure (C_c increases) caused by the formation-accumulation-diffusion towards the electrolyte bulk of the zinc corrosion products which have a dielectric constant significantly less than that of the free or associated water molecules. With regard to the zinc corrosion mechanism at the bottom of the thin coating pores, represented by the R_tC_{dl} and R_1C_1 time constants, it is thought that even if the reactions were kinetically different because the involved areas were smaller, the mechanism would be the same than the described for the Zn samples.

Analysis of the impedance spectra in terms of the equivalent circuit model of Fig. 6c allowed for the R_c and C_c, as well as R_t and C_{dl} parameters for ZPP samples were evaluated. Changes of these as a function of the exposure time to the electrolyte solution are plotted in Figs. 8a-8d. Within the first day of immersion the resistance R_c decreased quickly from about 1×10^8 Ω·cm^2 to ≈ 4.10^6 Ω·cm^2, Fig. 8a, while the capacitance C_c value remained at about 1×10^{-10} F·cm^{-2}, Fig. 8b. Accordingly to the also fast shift of the E_{corr} from -0.8 V/SCE to -0.92 V/SCE in the same lapse, it may be supposed that only a very small volume of electrolyte solution permeated through the organic coating structure and arrived to the zinc/coating interface. Then, during the whole test, the R_c values ranged from 10^6 Ω·cm^2 to 10^8 Ω·cm^2, i.e., equal or higher than the generally accepted value (10^6 Ω·cm^2) for protective coatings [102], while the corresponding to C_c (≈ 10^{-9}-10^{-10} F·cm^{-2}) were the characteristics of an intact paint coating, and demonstrative that it actually behaved like a dielectric capacitor throughout the immersion test. In summarize, the relatively good stability and protective properties inferred from the R_c and C_c values were interpreted as the variation of both the test solution resistivity and the geometric area in the

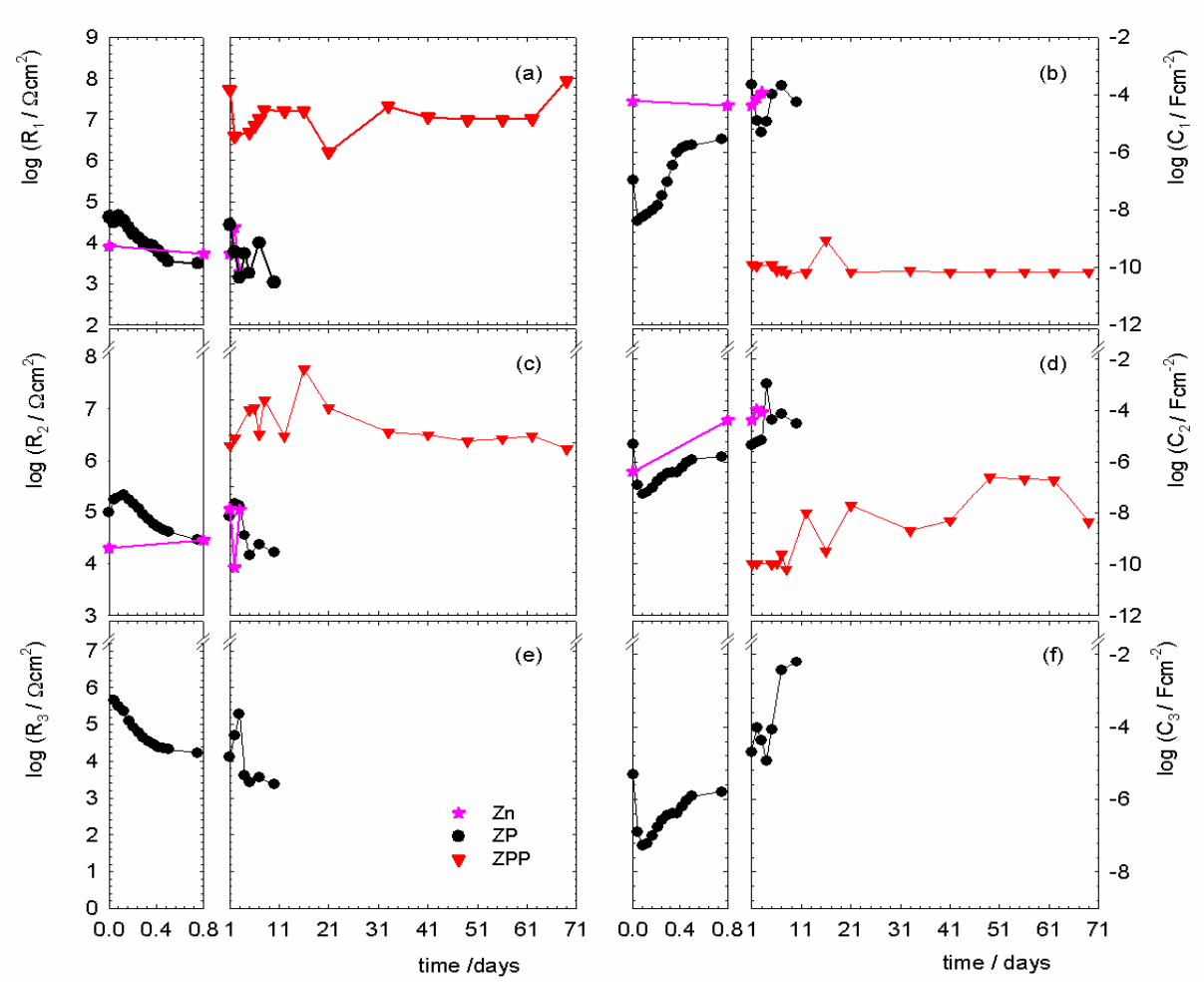

Fig. 8 Evolution of (a) log R_c, (b) log C_c,(c) log R_t, (d) log C_{dl}, (e) log R_1, (f) log C_1, impedance parameters, of ZP and ZPP samples at selected immersion times in aerated 0.05 mol·L^{-1} NaCl solution.

conducting pathways within the paint film related with the intact part of the same film was almost negligible along the test.

The experimental results plotted in Figs. 8c-8d support that probably due to the low (75 ± 5 μm) paint film thickness there was no induction period before the second time constant was identified at low frequencies. This time constant, R_tC_{dl}, was associated to a faradaic process whose contribution to the overall impedance of the tested samples was meaningful during the whole trial. As such period is related to the protective capacity of the paint coating, consequently, it is also associated to the delay to form the electrochemical double layer on the underlying metal surface. As can be seen in this figure, changes of the parameters governing the zinc corrosion process (R_t and C_c) took place mainly within the first 14 days of immersion with R_t values, which are inversely proportional to the corrosion rate, varying in the range 10^6-10^8 Ω·cm^2, Fig. 8c, and the corresponding to C_{dl} between 10^{-10} and 10^{-8} F·cm^{-2}, Fig. 8d. Since the values of these coupled parameters are inversely (R_t) and directly (C_{dl}) related to the electrochemically active area of the zinc substrate but their variations did not follow linearly this rule, it was assumed that during this period they could be affected by different areas instead of the total electrode area commonly used when the corresponding values are expressed by square centimetre [98]. The subsequent very slow deterioration process of the protective coatings up to the end of the test enabled that R_t started

to decrease from $\approx 7 \times 10^7\ \Omega \cdot cm^2$ to $1 \times 10^6\ \Omega \cdot cm^2$, while at the same time C_{dl} increased from $\approx 10^{-10}\ F \cdot cm^{-2}$ to $6 \times 10^{-7}\ F \cdot cm^{-2}$.

4. Conclusions

From the results generated during this investigation the following conclusions can be made with respect to the tested samples:

Dynamic system analysis with small perturbation allowed the determination of system specific parameters which characterize the deterioration of coated electrogalvanized steel with immersion time in 0.05 M NaCl solution. Also the water uptake in the early stage of exposure from the rate of changes in the paint dielectric capacitance was determined. Corrosion of painted/pre-treated electrogalvanized steel involves defect formation, penetration of corrodents, loss of adhesion, and attack of the substrate.

Even though in some cases the effects of different processes overlap, EIS showed to be a sensitive and reliable tool in evaluating the coated steel system degradation as a function of the immersion time and in monitoring the variations of the parameters associated to the physicochemical processes leading to such degradation. However, a simple qualitative analysis of the impedance spectra evolution could be too ambiguous to take out conclusions beyond the question. By this reason a proper fitting procedure as well as selection of the more significant electrical and electrochemical parameters was quite necessary.

All laboratory tests involved in this work were useful to characterize the bare or painted metallic surface allowing for understanding the behaviour of the studied system subjected to standardized (blistering, rusting, adhesion, porosity, gloss, colour, hardness, flexibility) as well as SEM, EDXS, and electrochemical (impedance spectra, corrosion potential) tests. Based on the good correlation between them, but mainly in the fact that they were demonstrative of the very slow deterioration rate of the barrier topcoat polyurethane paint/pre-treated electrogalvanized steel sheets/aerated 0.05 M NaCl solution, it was possible to assume that if a similar but thicker coating system is properly applied, it could be an acceptable alternative for protecting this type of substrate subjected to also similar exposure conditions.

Acknowledgments

The authors acknowledge CNPq (Process 490116/2006-0) of Brazil, CAPES/MINCyT (Process 158/09 of Brazil e BR/08/04 of Argentina), and Comisión de Investigaciones Científicas de la Provincia de Buenos Aires (CICPBA), Consejo Nacional de Investigaciones Científicas y Técnicas (CONICET) and Universidad Nacional de La Plata of Argentina for their financial support to this research.

References

[1] N. Zaki, Chromate conversion coating for zinc, Met. Finish. 86 (2) (1988) 75-76.

[2] R. Berger, U. Bexell, T.M. Grehk, S. Hörnström, A comparative study of the corrosion protective properties of chromium and chromium free passivation methods, Surf. Coat. Technol. 202 (2007) 391-397.

[3] N. Wen, Ch. Lin, Ch. Bai, M. Ger, Structures and characteristics of Cr(III)-based conversion coatings on electrogalvanized steels, Surf. Coat. Technol. 203 (2008) 317-323.

[4] C.R. Tomachuk, C.I. Elsner, A.R. Di Sarli, O.B. Ferraz, Corrosion resistance of Cr(III) conversion treatments applied on electrogalvanized steel and subjected to chloride containing media, Mat. Chem. Phys. 119 (2009) 19-29.

[5] C.R. Tomachuk, C.I. Elsner, A.R. Di Sarli, O.B. Ferraz, Morphology and corrosion resistance of Cr(III)-based conversion treatments applied on electrogalvanized steel, J. Coat. Technol. Research (2010). DOI: 10.1007/s11998-009-9213-1 (online).

[6] A.A.O. Magalhães, I.C.P. Margarit, O.R. Mattos, Molybdate conversion coatings on zinc surfaces, J. Electroanal. Chem. 572 (2004) 433-440.

[7] G.G. da Silva, I.C.P. Margarit-Mattos, O.R. Mattos, H. Perrot, B. Tribollet, V. Vivier, The molybdate-zinc conversion process, Corros. Sci. 51 (2009) 151-158.

[8] G.G. da Silva, A.N. Correia, P. de Lima-Neto, I.C.P. Margarit, O.R. Mattos, Study of conversion coatings obtained from tungstate-phosphoric acid solution, Corros. Sci. 47 (2005) 709-722.

[9] C. Stromberg, P. Thissen, I. Klueppel, N. Fink, G.

Grudmeier, Synthesis amd characterisation of surface gradient thin conversion films on zinc coated steel, Electrochim. Acta 52 (2006) 804-815.

[10] B.R.W. Hinton, Corrosion prevention and chromates: The end of an era, Met. Finish. 89 (1991) 55-61.

[11] B.R.W. Hinton, Corrosion prevention and chromates: The end of an era, Met. Finish. 89 (1991) 15-20.

[12] A. Barbucci, M. Delucchi, G. Cerisola, Study of chromate-free pre-treatment's and primers for the protection of galvanized steel sheets, Prog. Org. Coat. 33 (2) (1998) 131-138.

[13] T. Prosek, D. Thierry, A model for the release of chromate from organic coatings, Prog. Org. Coat. 49 (2004) 209-217.

[14] F. Deflorian, S. Rossi, L. Fedrizzi, P.L. Bonora, EIS study of organic coating on zinc surface pretreated with environmentally friendly products, Prog. Org. Coat. 52 (2005) 271-279.

[15] M.F. Montemor, A.M. Simões, M.G.S. Ferreira, C.B. Breslin, Composition and corrosion behaviour of galvanized steel treated with rare-earth salts: the effect of the cation, Prog. Org. Coat. 44 (2) (2002) 111-120.

[16] W. Trabelsi, P. Cecilio, M.G.S. Ferreira, M.F. Montemor, Electrochemical assessment of the self-healing properties of Ce-doped silane solutions for the pre-treatment of galvanized steel substrates, Prog. Org. Coat. 54 (4) (2005) 276-284.

[17] M.G.S. Ferreira, R.G. Duarte, M.F. Montemor, A.M.P. Simões, Silanes and rare earth salts as chromate replacers for pre-treatments on galvanized steel, Electrochim. Acta 49 (17-18) (2004) 2927-2935.

[18] T.L. Peng, R.L. Man, Rare earth and silane as chromate replacers for corrosion protection on galvanized steel, J. Rare Earths 22 (1) (2009) 159-163.

[19] X.H. Li, S.D. Deng, H.H. Fu, G.N. Mu, Synergistic inhibition effect of rare earth cerium (IV) ion and 3,4 dihydroxybenzaldehye on the corrosion of cold rolled in H_2SO_4 solution, Corros. Sci. 51 (2009) 2639-2651.

[20] J. Peultier, E. Rocca, J. Steinmetz, Zinc carboxylating: a new conversion treatment of zinc, Corros. Sci. 45 (8) (2003) 1703-1716.

[21] A.D. Apte, V. Tare, P. Bose, Extent of oxidation of Cr(III) to Cr(VI) under various conditions pertaining to natural environmental, J. Hazardous Mat. 128 (2006) 164-174.

[22] K. Ogle, S. Morel, N. Meddahi, An electrochemical study of the delamination of polymer coatings on galvanized steel, Corros. Sci. 47 (2005) 2034-2052.

[23] F. Deflorian, S. Rossi, P. Kamarchik, L. Fedrizzi, P.L. Bonora, Degradation mechanism of electrodeposited coatings in alkaline solutions, Prog. Org. Coat. 47 (2003) 103-111.

[24] M. Zapponi, C.I. Elsner, F. Actis, A.R. Di Sarli. Correlation between accelerated tests and outdoor exposure of coil-coated chromate and chromate free systems, Corros. Eng. Sci. and Technol. 44 (3) (2009) 119-127.

[25] G. Blustein, A.R. Di Sarli, J.A. Jaen, R. Romagnoli, B. del Amo. Study of iron benzoate: as a novel steel corrosion inhibitor pigment for protective paint films, Corros. Sci. 49 (2007) 4202-4231.

[26] M. Deyá, A.R. Di Sarli, B. del Amo, and R. Romagnoli. Performance of anticorrosive coatings containing tripolyphosphate in aggressive environments, Indust. & Eng. Chem. Research 70 (18) (2008) 7038-7047.

[27] B.M. Rosales, A.R. Di Sarli, O. de Rincón, A. Rincón, C.I. Elsner, B. Marchisio, et al., An evaluation of coil coating formulations in aggressive environments, Prog. Org. Coat., 50 (2) (2004) 105-114.

[28] B. del Amo, L. Véleva, C.I. Elsner, A.R. Di Sarli. Performance of coated steel systems exposed to different media: part I. painted galvanized steel, Prog. Org. Coat. 50 (3) (2004) 179-192.

[29] C.I. Elsner, E. Cavalcanti, O. Ferraz, A.R. Di Sarli. Evaluation of the surface treatment effect on the anticorrosive performance of paint systems on steel, Prog. Org. Coat. 48 (1) (2003) 50-62.

[30] L. De Rosa, T. Monetta, F. Bellucci, D.B. Mitton, A. Atienza, C. Sinagra, The effect of a conversion layer and organic coating on the electrochemical behavior of 8006 and 8079 aluminum alloys, Prog. Org. Coat. 44 (2002) 153-160.

[31] H.S. Emira, F.F. Abdel-Mohsen, The dependence of the corrosion protection of water-borne paints on the concentration of the anticorrosive pigment, Pigment & Resin Technol. 32 (4) (2003) 259-265.

[32] S.L. Bardage, J. Bjurman, Adhesion of waterborne paints to wood, J. Coat. Technol. 70 (878) (1998) 39-47.

[33] I. González, D. Mestach, J.R. Leiza, J.M. Asua, Adhesion enhancement in waterborne acrylic latex binders synthesized with phosphate methacrylate monomers, Prog. Org. Coat. 61 (2008) 38-44.

[34] T. Nabuurs, R.A. Baijards, A.L. German, Alkyd-acrylic hybrid systems for use as binders in waterborne paints, Prog. Org. Coat. 27 (1996) 163-172.

[35] O. Topçuoglu, S.A. Altinkaya, D. Balköse, Characterization of waterborne acrylic based paint films and measurement of their water vapor permeabilities, Prog. Org. Coat. 56 (2006) 269-278.

[36] E. Almeida, D. Santos, J. Uruchurtu, Corrosion performance of waterborne coatings for structural steel, Prog. Org. Coat. 37 (1999) 131-140.

[37] S. Ahmad, S.M. Ashraf, U. Riaz, S. Zafar, Development of novel waterborne poly(1-naphthylamine)/poly (vinylalcohol)-resorcinol formaldehyde-cured corrosion

resistant composite coatings, Prog. Org. Coat. 62 (2008) 32-39.

[38] M. Hernández, J. Genescá, J. Uruchurtu, F. Galliano, D. Landolt, Effect of an inhibitive pigment zinc-aluminum-phosphate (ZAP) on the corrosion mechanisms of steel in waterborne coatings, Prog. Org. Coat. 56 (2006) 199-206.

[39] S.K. Dhoke, A.S. Khanna, Effect of nano-Fe_2O_3 particles on the corrosion behavior of alkyd based waterborne coatings, Corros. Sci. 51 (2009) 6-20.

[40] F. Galliano, D. Landolt, Evaluation of corrosion protection properties of additives for waterborne epoxy coatings on steel, Prog. Org. Coat. 44 (2002) 217-225.

[41] A.C. Aznar, O.R. Pardini, J.I. Amalvy, Glossy topcoat exterior paint formulations using water-based polyurethane/acrylic hybrid binders, Prog. Org. Coat. 55 (2006) 43-49.

[42] M. Zubielewicz, W. Gnot, Mechanisms of non-toxic anticorrosive pigments in organic waterborne coatings, Prog. Org. Coat. 49 (2004) 358–371.

[43] T. Fujitani, Stability of pigment and resin dispersions in waterborne paint, Prog. Org. Coat. 29 (1996) 97-105.

[44] S. Kreutz, Mudanças e adaptações trazem menor toxicidade ambiental, Tintas & Vernizes 189 (2000) 24-28.

[45] R.E. Morgan, Zero VOC coating technology - Innovative solutions for old problems, Mater. Perform. 35 (1996) 31-36.

[46] B. Liu, Y. Li, H.C. Lin, Study on the anti-corrosion performance of acrylic-polyurethane, J. Chin. Soc. Corros. Prot. 23 (2003) 89-91.

[47] C.L. He, J.G. Deng, Y.S. Zhang, Polyurethane Ind., 17 (2002) 1-4.

[48] D.K. Chattopadhyay, K.V.S.N. Raju, Structural engineering of polyurethane coatings for high performance applications, Prog. Polym. Sci. 32 (2007) 352-418.

[49] M. Fratricova, P. Simon, P. Schwarzer, P. Wilde, Residual stability of polyurethane automotive coatings measured by chemiluminescence and equivalence of xenotest and solisi ageing tests, Polym. Degrad. Stabil. 91 (2006) 94-100.

[50] R.D. Armstrong, A.T.A. Jenkins, B.W. Johnson, An investigation into the UV breakdown of thermoset polyester coatings using impedance spectroscopy, Corros. Sci. 37 (10) (1995) 1615-1625.

[51] J.T. Zhang, J.M. Hu, J.K. Zhang, Studies of impedance models and water transport behaviors of polypropylene coated metals in NaCl solution, Prog. Org. Coat. 49 (2004) 293-301.

[52] Y. González-García, S. González, R.M. Souto, Electrochemical and structural properties of a polyurethane coating on steel substrates for corrosion protection, Corros. Sci. 49 (9) (2007) 3514-3526.

[53] L.X. Yang, X.G. Li, X.Q. Cheng, J. Chin. Soc. Corros. Prot. 26 (2006) 6-10.

[54] H. Marchebois, C. Savall, J. Bernard, S. Touzain, Electrochemical behavior of zinc-rich powder coatings in artificial sea water, Electrochem. Acta 49 (17-18) (2004) 2945-2954.

[55] ASTM B117-09, Standard practice for operating salt spray (fog) apparatus, 2009.

[56] DIN 50018, Testing in a saturated atmosphere in the presence of sulphur dioxide, 1997.

[57] DIN 50017, Atmospheres and their technical application condensation water test atmospheres, 1982.

[58] J.R. Mac Donald, Impedance Spectroscopy Emphasizing Solid State Materials, Ed. J. Wiley & Sons, New York, 1987.

[59] L. De Rosa, T. Monetta, D.B. Milton, F. Bellucci, Monitoring degradation of single and multilayer organic coatings, 1. absorption and transport of water: theoretical analysis and methods, J. Electrochem. Soc. 145 (11) (1998) 3830-3838.

[60] ASTM D 1210-05, Standard Test Method for fineness of dispersion of pigment-vehicle systems by Hegman-Tyoe Gage.

[61] ASTM D 3359-09e2, Standard test methods for measuring adhesion by tape test.

[62] ASTM D 5162-08, Standard practice for discontinuity (holiday) testing of nonconductive protective coating on metallic substrate.

[63] ASTM 523-08, Standard test methods for specular gloss.

[64] ASTM D 2244-11, Standard practice for calculation of color tolerances and color differences from environmentally measured color coordinates.

[65] ASTM 3363-11, Standard test methods for film hardness by pencil test.

[66] ASTM D 522-93A-08, Standard test methods for mandrel bend test of attached organic coatings.

[67] ASTM D-714-02/09, Standard Test for Evaluating Degree of Blistering of Paints, and ASTM D-610/08 Standard Practice for Evaluating Degree of Rusting on Painted Steel Surfaces, respectively.

[68] B.A. Boukamp, Equivalent Circuit, report CT88/265/128, CT89/214/128, University of Twente, The Netherlands, 1989.

[69] E.E. Schwiderke, A.R. Di Sarli, A mathematical basis for calculating the water permeability of organic films supported by metal substrates, Prog. Org. Coat. 14 (3) (1986) 297-308.

[70] T. Alfrey, E.F. Gurnee, W.G. Lloyd, Diffusion in glassy polymers, J. Polym. Sci. C 12 (1966) 249-261.

[71] N.M. Martyah, J.E. McCaskie, Surface structures of zinc chromate coatings, Met. Finish. 94 (2) (1996) 20-27.

[72] H. Leidheiser, J.W. Funke, Water disbondment and wet adhesion of organic coatings on metal: A review and interpretation, J. Oil Col. Chem. Assoc. 70 (5) (1987) 121-132.

[73] W. Schwenk, Corrosion Control by Organic Coatings, Leidheiser, H. Jr. Ed., NACE, Houston, TX, 1981, p. 103.
[74] T. Zsauer, A. Brandt, Impedance measurements on zinc-rich paints, J. Oil Col. Chem. Assoc. 67 (1) (1984) 13-17.
[75] D.J. Frydrych, G.C. Farrington, H. Townsend, Corrosion Protection by Organic Coatings, The Electrochemical Society, Pennington, NJ. 1987, p. 240.
[76] Rapports d'activite du laboratoire IVP Biennale 1975-1977, Internal Report of IVP, Belgium, p. 20.
[77] M. Piens, Importance of diffusion in the electrochemical action of oxidizing pigments, J. Coat. Technol. 51 (655) (1979) 66-73.
[78] Z.S. Smialowska, Passivity of Metals, The Electrochemical Soc. Corrosion Monographs Series, Princeton, NJ, 1978, p. 443.
[79] K.J. Vetter, Electrochem, Kinetics, Academic Press, NY, 1967, p. 754.
[80] A.S. Carpenter, Crystallinity in solid colloids. Solution and diffusion in high polymers, Trans. Faraday Soc. 43 (1947) 529-537.
[81] J.J. Ritter, J. Kruger, Corrosion Control by Organic Coatings, H. Leidheiser Jr., Ed., NACE, Houston, TX, 1981, p. 28.
[82] J. Wolstenholme, Electrochemical methods of assessing the corrosion painted metals-a review, Corros. Sci. 13 (7) (1973) 521-530.
[83] R.A. Armas, C. Gervasi, A.R. Di Sarli, S.G. Real, J.R. Vilche, Zinc rich paints on steels in artificial sea water by electrochemical impedance spectroscopy, Corrosion 48 (1992) 379-383.
[84] J.E.O. Mayne, The mechanism of the inhibition of the corrosion of iron and steel by means of paint, Official Digest 24 (1952) 127-136.
[85] M. Morcillo, R. Barajas, S. Feliú, J.M. Bastidas, A SEM study on the galvanic protection of zinc-rich paints, J. Mat. Sci. 25 (1990) 2441-2446.
[86] J.C. Hubrecht, J. Vereecken, Study of the anodic and cathodic corrosion process of coated iron with the ac impedance technique, in: Proc. 9th Int. Cong. On Metallic Corrosion, Toronto, 1984, pp. 85-90.
[87] D.E. Williams, J. Asher, Measurement of low corrosion rates: Comparison of A.C. impedance and thin layer activation methods, Corros. Sci. 24 (1984) 185-196.
[88] C. Cachet, U. Ströder, R. Wiart, The kinetics of zinc electrode in alkaline zincate electrolyte, Electrochim. Acta 27 (7) (1982) 903-908.
[89] L. Fedrizzi, L. Ciaghi, B.L. Bonora, R. Fratesi, G. Riventi, Corrosion behavior of electrogalvanized steel in sodium chloride and ammonium sulphate solutions, a study by EIS, J. Appl. Electrochem. 22 (3) (1992) 247-254.
[90] C. Cachet, R. Wiart, The kinetics of zinc dissolution in chloride electrolytes: Impedance measurements and electrode morphology, J. Electroanal. Chem. 111 (2-3) (1980) 235-246.
[91] C. Cachet, R. Wiart, Reaction mechanism for zinc dissolution in chloride electrolytes, J. Electroanal. Chem. 129 (1-2) (1981) 103-114.
[92] X.G. Zhang, Corrosion and Electrochemistry of Zinc, Plenum Press, New York, 1996, pp. 32-33.
[93] O. Ferraz, E. Cavalcanti, A.R. Di Sarli, Characterization of protective properties for some naval steel/polymeric coating/3% NaCl solution systems by EIS and visual assessment, Corros. Sci. 37 (8) (1995) 1267-1280.
[94] P.R. Seré, D.M. Santágata, C.I. Elsner, A.R. Di Sarli, The influence of the method of application of the paint on the corrosion of the substrate as assessed by ASTM and electrochemical method, Surf. Coat. Intern. 3 (1998) 128-134.
[95] D.M. Santágata, P.R. Seré, C.I. Elsner, A.R. Di Sarli, Evaluation of the surface treatment effect on the corrosion performance of paint coated carbon steel, Prog. Org. Coat. 33 (1998) 44-54.
[96] P.R. Seré, A.R. Armas, C.I. Elsner, A.R. Di Sarli, The surface condition effect on adhesion and corrosion resistance of carbon steel/chlorinated rubber/artificial sea water systems, Corros. Sci. 38 (6) (1996) 853-866.
[97] H. Leidheiser, J., M.W. Kendig, The mechanism of corrosion of polybutadiene coated steel in aerated sodium chloride, Corrosion 32 (1976) 69-75.
[98] G.G. Nascimento, O.R Mattos, J.L. Santos, I.C.P. Margarit, Impedance measurements on lacquered tinplate: fitting with equivalent circuits, J. Appl. Electrochem. 29 (1999) 383-392.
[99] C. Cachet, V. Ströder, R. Wiart, Impedance measurements during the cycling of a zinc electrode, J. Appl. Electrochem. 11 (1981) 613-623.
[100] E. Almeida, D. Pereira, O. Figueiredo, The degradation of zinc coatings in salty atmospheres, Prog. Org. Coatings 17 (2) (1989) 175-189.
[101] W.J. Lorenz, F. Mansfeld, Determination of corrosion rates by electrochemical DC and AC methods, Corros. Sci. 21 (9-10) (1981) 647-672.
[102] J.R. Vilche, E.C. Bucharsky, C.A. Giúdice, Application of EIS and SEM to evaluate the influence of pigment shape and content in ZRP formulations on the corrosion prevention of naval steel, Corrosion Science 44 (2002) 1287-1308.